THE JOURNAL OF PHYSICAL CHEMISTRY B

Article

pubs.acs.org/JPCB

Effect of Hydrophobic Interactions on the Folding Mechanism of β-Hairpins

Alexander Popp,[†] Ling Wu,[§] Timothy A. Keiderling,*[,§] and Karin Hauser*[,†]

[†]Biophysical Chemistry, Department of Chemistry, University of Konstanz, 78457 Konstanz, Germany

[§]Department of Chemistry, University of Illinois at Chicago, 845 West Taylor Street, Chicago, Illinois 60607-7061, United States

Supporting Information

ABSTRACT: Hydrophobic interactions are essential in stabilizing protein structures. How they affect the folding pathway and kinetics, however, is less clear. We used time-resolved infrared spectroscopy to study the dynamics of hydrophobic interactions of β-hairpin variants of the sequence Trpzip2 (SWTWENGKWTWK-NH2) that is stabilized by two cross-strand Trp−Trp pairs. The hydrophobicity strength was varied by substituting the tryptophans pairwise by either tyrosines or valines. Relaxation dynamics were induced by a laser-excited temperature jump, which separately probed for the loss of the cross-strand β-hairpin interaction and the rise of the disordered structure. All substitutions tested result in reduced thermal stability, lower transition temperatures, and faster dynamics compared to Trpzip2. However, the changes in folding dynamics depend on the amino acid substituted for Trp. The aromatic substitution of Tyr for Trp results in the same kinetics for the unfolding of sheet and growth of disorder, with similar activation energies, independent of the substitution position. Substitution of Trp with a solely hydrophobic Val results in even faster kinetics than substitution with Tyr but is additionally site-dependent. If the hairpin has a Val pair close to its termini, the rate constants for loss of sheet and gain of disorder are the same, but if the pair is close to the turn, the sheet and disorder components show different relaxation kinetics. The Trp → Val substitutions reveal that hydrophobic interactions alone weakly stabilize the hairpin structure, but adding edge-to-face aromatic interaction strengthens it, and both modify the complex folding process.

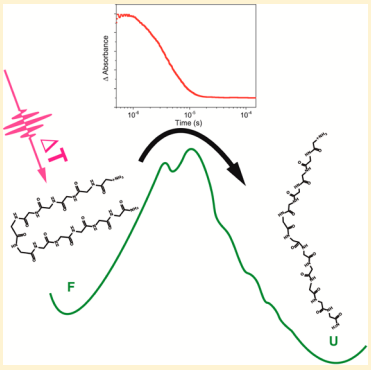

INTRODUCTION

Hydrophobic interactions play a fundamental role in protein folding mechanisms. Many folding processes are driven by a hydrophobic collapse that precedes and facilitates the formation of secondary structure elements. However, quantification of the hydrophobic-driven contribution to the folding process is difficult. Studies of small peptides with a well-defined secondary structure, ideally suited to analyze folding dynamics of β-sheet like structures at the residue level, have often focused on tryptophan zipper peptides ("Trpzip"), which were designed by Cochran and co-workers to form β-hairpins.[1] The two cross-strand Trp−Trp pairs are in alternate sequential positions so that they lie on one side of the hairpin and stabilize the β-hairpin structure by the aromatic indole rings forming two favored edge-to-face interactions.[2] By contrast, polar groups in the sequence and the turn promote solubility.[3]

The folding mechanism of the Trpzip2 sequence (SWTWENGKWTWK-NH2) with an aspargine−glycine (NG) turn has been intensively studied by time-resolved measurements that all indicate a multistate process.[4−10] One way to probe the details of the folding mechanisms is by use of infrared (IR) spectroscopic detected relaxation dynamics after a laser-excited temperature jump (T-jump), which allows separate analyses of conversion between conformations in the peptide. IR T-jump-detected kinetics have proven to be a powerful approach to get insights into the folding mechanisms even in the context of a larger protein fold.[11]

In this study, we analyze the impact of specific hydrophobic interactions on the formation of a β-hairpin structure by mutations of the Trpzip2 sequence to alter the cross-strand alignment of residues (Scheme 1). The hydrophobicity was modified by substituting tryptophans with either tyrosines (aromatic and hydrophobic) or valines (solely hydrophobic). Previous thermodynamic analyses of equilibrium FTIR and CD measurements as well as NMR studies have shown that these mutant peptides are destabilized with respect to Trpzip2, resulting in a reduced transition temperature, but in most cases they can still form a β-hairpin structure.[12−14] Our previous NMR studies showed that, when substituted for Trp in Trpzip2, Tyr forms edge-to-face interactions with other Tyr or Trp aromatic side chains. This interaction has been shown to result in circular dichroism (CD) spectra characterized by a strong couplet shape centered at ∼220 nm that arises from coupling of the indol ^1B_b transitions.[15] The β-hairpins formed were strongly twisted, with the exception of the mutant that has cross-strand Tyr−Trp interactions which was somewhat flatter, and all exhibited somewhat distorted Type I′ turns.[3,12,13] The

Received: July 3, 2014
Revised: November 12, 2014
Published: November 13, 2014

   dx.doi.org/10.1021/jp506658x | J. Phys. Chem. B 2014, 118, 14234−14242

Scheme 1[a]

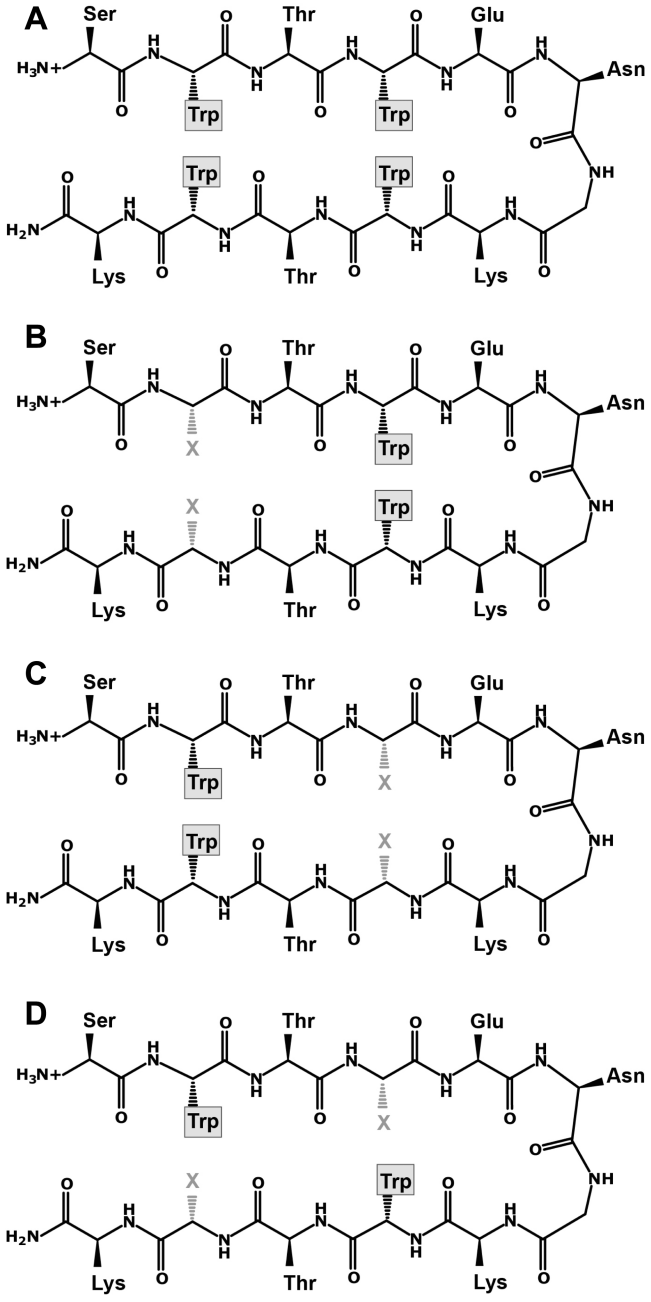

[a](A) Tripzip2 sequence with the four tryptophans on positions 2, 4, 9, and 11 forming the hydrophobic core; mutant variants follow in the order (B) XWWX, (C) WXXW, and (D) WXWX, which have one tryptophan pair exchanged with either tyrosines (Y) or valines (V) on positions marked with X.

analyses of the Tyr mutants' spectral behavior showed the three variants studied to be relatively consistent and have similar transition temperatures as monitored by FTIR (secondary structure) or CD (cross-strand aromatic interactions). However, the Val mutants showed different CD and FTIR transitions, which indicates a difference in stability for the backbone and residual aromatic interaction. In addition, the Val mutants only folded if the structure maintained a direct cross-strand Trp−Trp interaction; the Val−Trp interaction was insufficient for folding.

As an extension of our previous equilibrium studies to now incorporate analyses and comparison of dynamics, we here present results of laser-induced temperature-jump measurements that differentiate two aspects of hydrophobic interactions contributing to the hairpin folding dynamics. We determined relaxation times for several Trpzip2-like peptides with pairwise mutations of the tryptophans at different positions in the β-hairpin structure (as shown in Scheme 1). This allowed identification of the impact of specific types and locations of hydrophobic residues on the folding mechanism. To the best of our knowledge, this is the first time that effects of aromatic versus just hydrophobic cross-strand interactions on dynamics of tight hairpin structure formation have been measured and distinguished at the residue level in order to explore their role in modifying folding pathways. Some earlier studies have done Trp → Tyr → Ala mutations on hairpins with larger turns (i.e., Trpzip4) but used single residue mutants, not the cross strand interactions we focus on here.[16]

EXPERIMENTAL SECTION

Peptide Synthesis and Sample Preparation. All tyrosine mutant peptides were synthesized at the University of Illinois at Chicago (UIC) using standard Fmoc-based solid-state synthesis methods, but the valine mutants were obtained commercially (GenScript Corp.), as was described previously.[12,13] Crude peptides were purified by reverse-phase HPLC (VYDAC 218TP510 reversed-phase column) and characterized by MALDI-MS. For IR samples, the peptides were dissolved in 0.1 M DCl and lyophilized three times to remove residual trifluoroacetic acid (TFA), which absorbs at ~1672 cm^{-1} and interferes with the amide I IR absorbance region. The peptides were dissolved at 20 mg/mL in D_2O (pD ~ 1.5, using standard correction of adding 0.4 to measured pH). The IR cells are composed of two CaF_2 windows separated by a 100 μm Teflon spacer corresponding to the optical path length of the cell.

FTIR Studies in Thermal Equilibrium. The thermal unfolding behavior of the peptide variants was determined from the temperature-dependent IR spectra measured with an Equinox 55 FTIR (Bruker, Germany) using an MCT detector and spectral resolution of 4 cm^{-1}. The amide I band was used as a vibrational probe for secondary structure (termed amide I′ when D_2O is used as solvent instead of H_2O). Spectra were collected as an average of 128 scans with ΔT = 5 °C steps over the range from 5 to 85 °C, for both the peptide solution and the D_2O reference measured sequentially using a homemade temperature-controlled shuttle device that is connected to a water bath (Lauda Ecoline E300, Germany). The switching between the two cells and the data collection were automated to allow for equilibration after each temperature step. The actual temperature in the cell was monitored by a Pt100 temperature sensor to ensure a precise control. The transition temperatures were derived from a fit to a two-state model of the change in amide I′ intensity (Supporting Information).

Time-Resolved Temperature-Jump Measurements. The measurements of the relaxation kinetics were performed with a home-built T-jump spectrometer. Rapid heating of the solvent was induced by a Q-switched Nd:YAG laser pulse (5 ns, 700 mJ at 1064 nm, Continuum, Excel Technology, Europe) whose 1909 nm Raman-shifted component excites an overtone vibration of D_2O. The Raman shifter (Radiant Dyes, Germany) contains H_2 gas at 30 bar. The pump pulse was split into two counter propagating beams to provide more homogeneous

dx.doi.org/10.1021/jp506658x | J. Phys. Chem. B 2014, 118, 14234−14242

Table 1. Peptide Sequences

peptide[a]	sequence	T_m (K) at neutral pH[c]	T_m (K) at acidic pH[c]
WWWW (Trpzip2)	SWTWENGKWTWK-NH_2	352 ± 3[12]	340 ± 1[12]
WWWW (Trpzip2C)	AWAWENGKWAWK-NH_2	340 ± 1[17]	337 ± 5[10]
WYWY	SWTYENGKWTYK-NH_2	338 ± 2[13]	341 ± 1
WYYW	SWTYENGKYTWK-NH_2	331 ± 2[13]	320 ± 1
YWWY	SYTWENGKWTYK-NH_2	331 ± 4[13]	322 ± 1
WVVW[b]	SWTVENGKVTWK	332 ± 2[12]	317 ± 4[12]
VWWV[b]	SVTWENGKWTVK	326 ± 7[12]	311 ± 4[12]

[a]Specified residues are on positions 2, 4, 9, 11. [b]In previous studies, WVVW and VWWV were termed W2W11 and W4W9, respectively. [c]Monitored with FTIR equilibrium measurements.

heating of the sample and to reduce cavitation problems by use of a (5 ns) delay between them.[18] Additionally, a beam homogenizer (SUSS MicroOptics, Germany) was inserted into each pump beam to reduce hot spots due to the nonlinear effects in the Raman-shifting process. This addition provided a more uniform heat distribution in the pumped volume. The size of the temperature jump can be varied by the intensity of the pump pulse. To produce a T-jump of ∼7 °C the energy of the 1909 nm beam was about 50 mJ focused to a spot size of ∼1 mm diameter at the sample position. A quantum cascade laser (QCL, Daylight Solutions Inc., U.S.A.) provided a tunable cw light source used as the IR probe. The usable spectral range for this QCL lies between 1715 and 1580 cm^{-1}, which covers the whole amide I region. The probe beam was focused to a diameter of ∼200 μm at the center of the sample heated area. The sample was equilibrated at a defined temperature by flow from a water bath connected to the cell holder. Relaxation kinetics were determined from the change in transmission measured at selected amide I′ frequencies using a photovoltaic MCT detector (18 MHz, KMPV11−1-J2, Kolmar Technologies, Newburyport, MA, U.S.A.). The transients were digitized with a 16 bit transient recorder board (Spectrum, Germany).

Data Analysis of the T-Jump Studies. In order to determine the relaxation times of the investigated peptide, ∼2000 transients were averaged. Each data set was preprocessed to filter out those transients distorted due to cavitation effects using a program written in-house (MATLAB2010, The MathWorks, MA, U.S.A.). The observed transients comprise both peptide and solvent dynamics. We used a biexponential fit ($\Delta A(t) = A_0 + A_1 \exp(-t/\tau_1) + A_2 \exp(-t/\tau_2)$) to decompose the kinetics of the peptide relaxation and the solvent cooling, each corresponding to independent monoexponential decay functions (ORIGIN, OriginLab, MA, U.S.A.). The time interval analyzed for the fit was based only on the data points between 500 ns to 200 μs, because signal perturbations due to thermal lensing effects and electronic detector ringing are observable at <500 ns and because the cooling of the solvent becomes strongly nonexponential for time scales >200 μs. (The water cooling time constant is >150 μs and has no distortion impact on the fast hairpin dynamics we measure.) The size of the applied temperature jump was determined by the apparently instantaneous change in the absorbance signal ΔA after the laser trigger. This may be slightly overestimated due to additional temperature-dependent absorbance changes of the peptide, but the error is probably ≤1 °C. The peptide temperature after the T-jump was calculated by referencing to the temperature-dependent FTIR absorption spectra of D_2O measured in thermal equilibrium and taking the initial peptide temperature and probed wavenumber into account.

RESULTS AND DISCUSSION

Mutations in the Hydrophobic Core. The 12 amino acid peptide Trpzip2 (SWTWENGKWTWK) contains four tryptophans (W) on positions 2, 4, 9, and 11 that form cross-strand pairs and is designated as **WWWW** (Table 1). The mutant peptides vary by the substitution of two tryptophans at different positions (Scheme 1 and Table 1). Either aromatic tyrosines or aliphatic valines are substituted for the cross-strand tryptophan pair close to the turn on positions 4 and 9 to give (**WYYW**) or (**WVVW**), respectively, or alternately for the cross-strand tryptophan pair close to the hairpin termini on positions 2 and 11 giving (**YWWY** or **VWWV**). Another variant has been studied that has an alternating cross-strand Trp/Tyr pair (**WYWY**). This latter peptide forms a well-defined β-hairpin, whereas the analogous alternating Trp/Val pair (**WVWV**) has a more disordered structure and was not analyzed. Equilibrium FTIR and CD studies and NMR structures of the mutant peptides have been reported previously.[12,13] Table 1 summarizes the transition temperatures of the peptide variants derived from FTIR studies at neutral and acidic pH.[10,12,13,17] Mutations in the hydrophobic core of Trpzip2 lead to a lower T_m, indicating their lower structural stability. At acidic pH, the peptide is less stable, and the T_m values consistently shift to lower values. The mutant transition temperatures decrease significantly from the **WWWW** value for **WYYW** and **YWWY** but less so for the cross mutant, **WYWY**. The valine variant **WVVW** has a thermal stability similar to that of **WYYW** and **YWWY**, whereas the **VWWV** variant has the lowest T_m. The solubility is enhanced at low pH resulting in a more reliably reversible thermal transition. Thus, low pH conditions were chosen for the T-jump measurements because several thousand transients have to be averaged for the kinetic analysis. The pH might influence the absolute values of the relaxation times. However, all T-jump measurements were performed at the same pH conditions, and thus, the comparisons of relaxation times determined for the various peptide variants reflect the impact of the mutation. Trpzip2C is a variant of Trpzip2 having three alanine mutations on positions 1, 3, and 10 but otherwise has the same amino acid sequence. In particular, Trpzip2C maintains the hydrophobic core with the four tryptophans on positions 2, 4, 9, and 11 (Table 1). The alanine mutations have virtually no impact on the kinetics as evidenced by a comparison of our T-jump studies on Trpzip2C and the T-jump IR data of Trpzip2 from other groups.[5,8] Trpzip2C is used as the **WWWW** reference in this study, because we have obtained relaxation rates for it over a large temperature range.[9,10]

Probing Structural Dynamics. Based on the temperature-induced FTIR equilibrium unfolding studies, representative amide I′ frequencies were chosen to best probe conformation-

dx.doi.org/10.1021/jp506658x | J. Phys. Chem. B 2014, 118, 14234−14242

ally specific structural dynamics that primarily reflect β-hairpin cross-strand formation (~1628 cm^{-1}) and change of the disordered component (1663 cm^{-1}). Figure 1 shows, as an example, the FTIR equilibrium measurements for one of the peptides studied (WYWY). The amide I′ reveals a frequency shift and intensity variation at the selected frequencies upon heating the sample that correspond to aspects of the folding/unfolding transition. Representation of the thermal variation of the FTIR as difference spectra highlights the frequency positions for the maximum intensity changes (1628 and 1663 cm^{-1}), which in turn are used as probe frequencies for the T-jump studies. The transition temperatures for all peptide variants studied, as determined from these spectra, are summarized in Table 1. Relaxation kinetics were monitored after the laser-induced T-jump starting at various peptide temperatures.

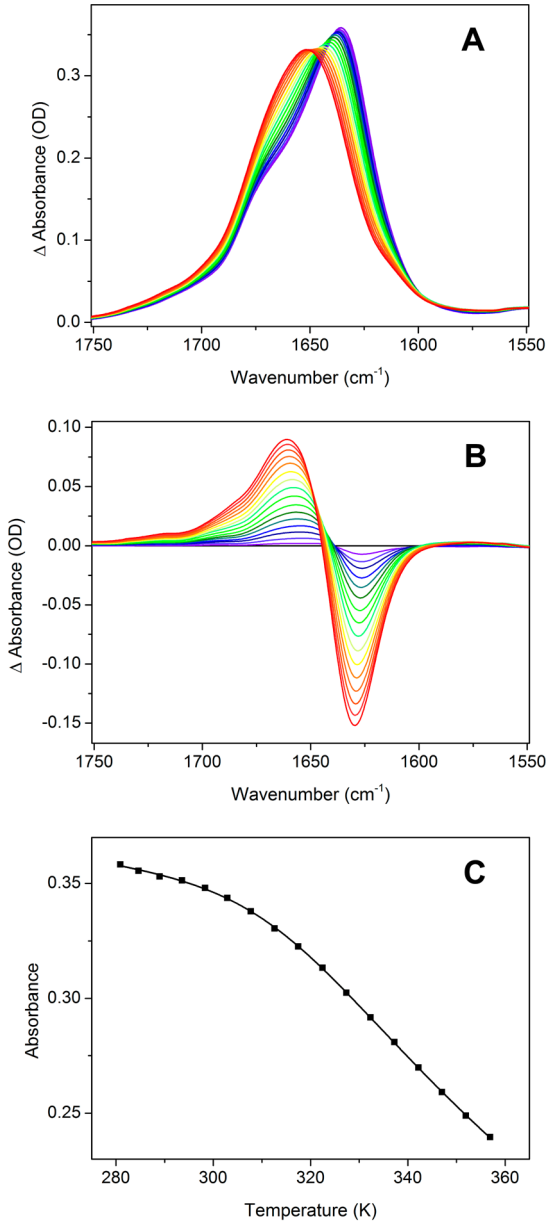

Figure 1. FTIR thermal equilibrium data for one of the tyrosine mutants (**WYWY**) at acidic pH. A: Amide I′ absorption varying from 5 °C (blue) to 85 °C (red) in steps of 5 °C. B: Difference spectra, obtained by subtracting the spectrum at 5 °C from the higher temperature spectra. The decrease at ~1628 cm^{-1} represents the loss of β-hairpin, whereas the increase at ~1663 cm^{-1} is correlated to the rise of disordered structure. C: Analysis of the unfolding transition represented as a plot of the intensity at 1628 cm^{-1} versus temperature.

Figure 2 shows example transient absorbances for the same **WYWY** variant probed at 1628 cm^{-1} (decay of the β-hairpin structure) and 1663 cm^{-1} (rise of the disordered structure). The transients were fit as described in the Experimental Section, and relaxation times were determined as a function of temperature. Some conclusions can be immediately drawn from this single example. The loss of sheet (blue data) and the gain of disorder (red data) are fast processes but have similar time constants (~1.3 μs), which is in contrast to the previously reported data for **WWWW**.[9] To get insights about how these kinetics might vary with position and type of substitution, we present T-jump data for the Tyr and Val mutants below. Example transients for all mutants can be found in Supporting Information and selected time constants in Table 2.

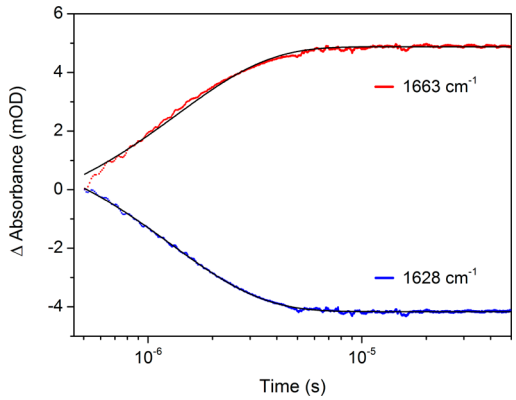

Figure 2. Laser-excited T-jump relaxation kinetics probed at 1663 cm^{-1} (red, sensing dynamics of the growth of disordered structure) and 1628 cm^{-1} (blue, β-hairpin decay dynamics) for **WYWY** (with a final peptide temperature after the temperature jump of T = 46.5 °C). Data shown are for the measured transient after subtraction of the varying D_2O contribution, as obtained from the biexponential fit.

Tyrosine Mutants. There is a strong impact on the Trpzip2 kinetic behavior and temperature dependence when tryptophans are substituted by tyrosines. The relaxation times for the three mutants, **WYYW**, **YWWY**, and **WYWY**, measured at various temperatures decrease with increasing temperature over the range studied (selected values listed in Table 2), as would be expected for normal Arrhenius behavior. In contrast to the **WWWW** hairpin, the dynamics for the β-strand decay (1628 cm^{-1}) and rise of disordered structure (1663 cm^{-1}) yield almost the same values for all three mutants. The virtual overlap in the variation in their rate constants over the temperature range is shown in Figure 3. Apparent activation energies for this potentially multistep process were determined (listed in Table 3) from the temperature dependence of these Arrhenius plots but will be referred to as activation energies for simplicity.

As clearly shown in Figure 3, the relaxation kinetics of the loss of β-strand (1628 cm^{-1}) and gain of disorder (1663 cm^{-1}) behave equivalently in terms of activation energy for all tyrosine mutants, but they have some variation in pre-exponential factor. Only the relaxation rates of **YWWY** probed at 1628 cm^{-1} and at high temperatures (>45 °C) deviate from the common slope

dx.doi.org/10.1021/jp506658x | J. Phys. Chem. B 2014, 118, 14234−14242

Table 2. Relaxation Times (μs) at Selected Peptide Temperatures[a,b]

	1628 cm^{-1}				1663 cm^{-1}			
	10 °C	25 °C	40 °C	55 °C	10 °C	25 °C	40 °C	55 °C
WYWY	6.7 (13 °C)	3.5 (24 °C)	1.6 (41 °C)	0.7 (57 °C)	7.3 (9 °C)	3.1 (25 °C)	1.7 (40 °C)	0.9 (55 °C)
WYYW	7.5 (9 °C)	3.0 (27 °C)	1.7 (38 °C)	0.6 (55 °C)	6.7 (10 °C)	2.5 (27 °C)	1.4 (41 °C)	0.5 (55 °C)
YWWY	6.0 (10 °C)	2.6 (25 °C)	1.2 (40 °C)	0.3 (56 °C)	6.4 (10 °C)	2.6 (25 °C)	1.2 (39 °C)	0.5 (54 °C)
WVVW	3.8 (11 °C)	3.0 (25 °C)			6.5 (10 °C)	2.7 (25 °C)	1.4 (39 °C)	0.9 (55 °C)
VWWV	3.5 (11 °C)	1.3 (24 °C)	0.6 (36 °C)		3.7 (10 °C)	1.5 (25 °C)		

[a]Values refer to the nominal, targeted final peptide temperatures after the T-jump; numbers in brackets indicate the temperature values actually measured in each experiment. [b]The statistical error in fitting the transients is low (10–20 ns), but the experimental (reproducibility) error for repeated transients is in the range of 150 ns.

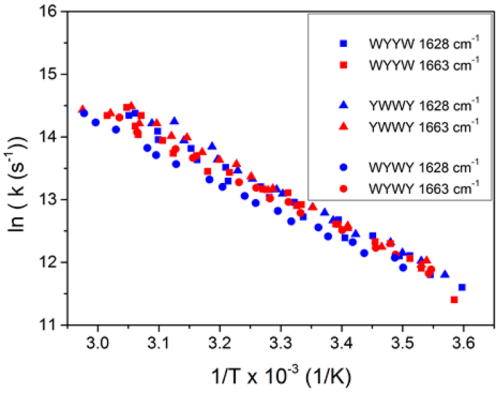

Figure 3. Arrhenius plots of the temperature dependence of the relaxation rate constants for the tyrosine mutants (**YWWY**, **WYYW**, **WYWY**). The temperature refers to the final peptide temperature after the temperature-jump. Activation energies were determined by $\ln(k) = -E_a/(RT) + \ln(A)$ and are listed in Table 3.

and increase significantly (data not shown). We have eliminated this data (although reproducible) from the fit and Figure 3 due to their lower reliability. The remaining data have the same Arrhenius slopes for all the tyrosine mutants. Consequently, the activation energies determined for the hairpin decay and the rise of the disordered structure deviate only slightly (Table 3).

Table 3. Apparent Activation Energies (kJ/mol)

variant	probe ν	E_a
WWWW	1625 cm^{-1}	27.8 ± 2.3
	1661 cm^{-1}	33.2 ± 1.4
WYYW	1628 cm^{-1}	43.4 ± 1.1
	1663 cm^{-1}	40.5 ± 1.2
YWWY	1628 cm^{-1}	42.7 ± 1.0
	1663 cm^{-1}	40.5 ± 1.1
WYWY	1628 cm^{-1}	38.2 ± 0.7
	1663 cm^{-1}	39.2 ± 0.5
VWWV	1628 cm^{-1}	46.9 ± 1.5
	1663 cm^{-1}	43.2 ± 2.3
WVVW	1628 cm^{-1}	12.8 ± 1.4
	1663 cm^{-1}	33.8 ± 1.0

Although the relaxation times for **WYWY** probed at 1628 cm^{-1} tend to be systematically slower than for the other Tyr mutants (Table 2), the effect on the Arrhenius slope is marginal. The **WYWY** variant shows the smallest deviation in activation energies for change in the two monitored structural components, strand and disorder, 38.2 kJ/mol (1628 cm^{-1}) and 39.2 kJ/mol (1663 cm^{-1}), respectively. This apparent two-state behavior for the Tyr substituted variants stands in contrast to the **WWWW** stabilized parent hairpin where the relaxation times for loss of strand and gain of disorder clearly differ from each other in the low temperature region but tend to merge at higher temperatures.[9]

Valine Mutants. By contrast to the Tyr results above, the two Val mutants studied (**WVVW**, **VWWV**) show different conformational dynamics from each other (as shown in the separate Arrhenius plots in Figure 4). The **VWWV** variant (Trp

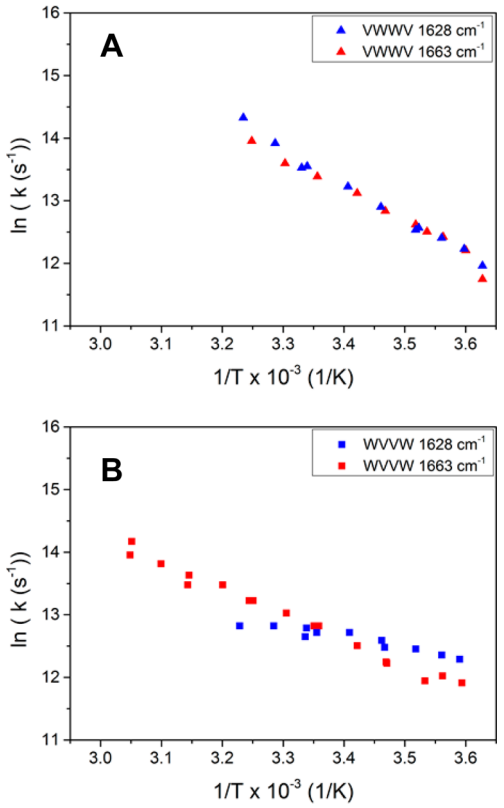

Figure 4. Arrhenius plots for the valine mutants (A) **VWWV** and (B) **WVVW** probed at the two wavenumbers (1628, blue, and 1663 cm^{-1}, red) characteristic of strand and disorder.

pair substituted with Val closer to the hairpin termini) has the lowest transition temperature of all the peptides studied (Table 1) and the fastest relaxation times (Table 2), which are virtually equivalent for dynamics probed at 1628 cm^{-1} (strand) and 1663 cm^{-1} (disordered structure). In contrast to **VWWV**, the relaxation times of **WVVW** (which has Val substituted for the Trp pair adjacent to the turn) differ for the strand and disordered structure in at least the low temperature region (<25 °C). The strand decay is faster than the rise of disordered

dx.doi.org/10.1021/jp506658x | J. Phys. Chem. B 2014, 118, 14234–14242

structure at low temperatures, whereas at higher temperatures the relaxation times tend to become similar. This is qualitatively the same pattern that was seen with **WWWW** but with faster relaxation times, as compared in Figure 5.[9,10] Unfortunately, we

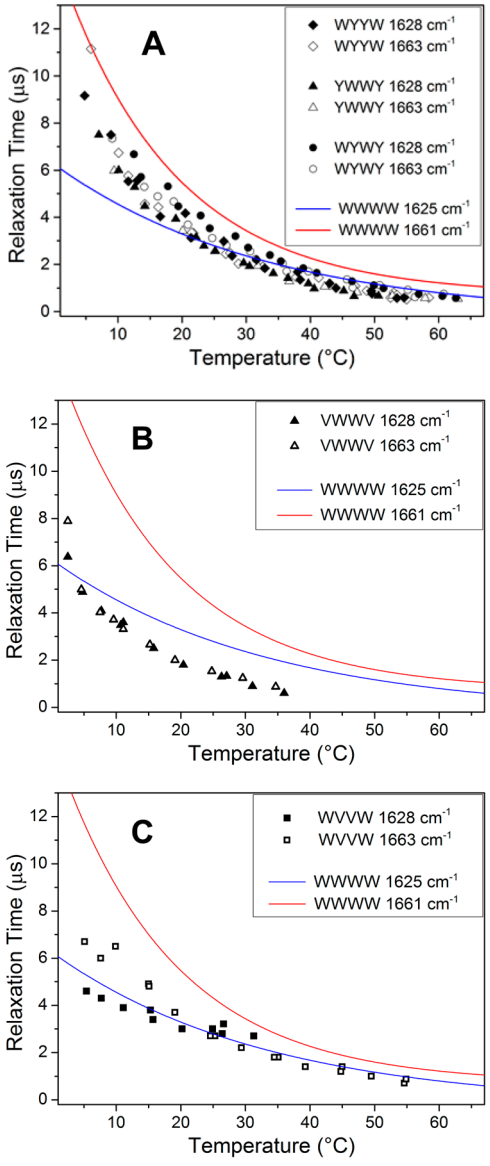

Figure 5. Impact of hydrophobic interactions on the dynamics. Comparison of the relaxation times between the various mutant peptides (black) and the **WWWW** variant Trpzip2C (whose data points are eliminated for clarity and represented with colored lines from the fits). A: **WYYW**, **YWWY**, **WYWY**; B: **VWWV**; C: **WVVW**.

could not measure reliable data for temperatures above 30 °C for **WVVW** because the absorbance changes are very small when probed at 1628 cm^{-1}, and cavitation effects become more of a problem at higher peptide temperatures in general. (This also affects both measurements for **VWWV**.) From the thermodynamic point of view, **WVVW** has a higher T_m than **VWWV**. Concerning the relaxation times, the strand decay (1628 cm^{-1}) of **WVVW** is similar to that of the **WWWW** variant but is not as fast as for the **VWWV** variant. The 1661 cm^{-1} dynamics of **WVVW** is also slower than for **VWWV**, but in this case, it was similar to that of the tyrosine mutants (Table 2 and Figure 5).

Conformational Dynamics Driven by Hydrophobic Interactions. In previous T-jump studies, we showed that at lower temperatures (<40 °C) the Trpzip2C (**WWWW**) hairpin has slower relaxation times for growth of the disordered structure in comparison to loss of the β-strand.[9,10] Even though the strong Trp−Trp interactions remain largely intact at these low temperatures, residue-specific conformational changes of the peptide backbone were identified using isotope labeling that revealed the contribution of intermediate states having partial loss of cross-strand H-bonding both at the termini and near the turn. Considering our mutations, Val has a significantly higher hydrophobicity than Trp or Tyr, while those are similar in hydrophobicity.[19] Trp and Tyr both have aromatic side chains with heteroatom functionality, which are capable of forming hydrogen bonds, but more importantly which can enhance structural stability by either ring stacking or, in this case, edge-to-face interactions. In contrast, Val has an aliphatic side chain that cannot form hydrogen bonds or develop dipolar interaction. The aromatic edge-to-face interaction between cross-strand pairs appears critical for stabilization of the hairpin structure because there is a fundamental difference in stability between the alternate variants, **WYWY** and **WVWV**; **WYWY** forms a stable (and less twisted) β-hairpin structure, whereas **WVWV** is mostly disordered.[12,13] On the other hand, one aromatic cross-strand pair is sufficient to stabilize a hairpin structure at low temperature as seen with the **WVVW** and **VWWV** variants.[12] The T_m of **WVVW** is even similar to that of the **WYYW** and **YWWY** variants, which are stabilized by two aromatic cross-strand pairs. Interestingly, the alternate variant **WYWY** reveals the highest T_m among the three tyrosine mutants, its value being significantly higher than for **WYYW** and **YWWY**.

Comparing the activation energies (Table 3), only the **WVVW** variant shows clearly different values for the hairpin decay (12.8 kJ/mol) and the rise of disordered structure (33.8 kJ/mol), as was also the case for the **WWWW** stabilized Trpzip2. All other variants (**WYYW**, **YWWY**, **WYWY**, **VWWV**) have experimentally equivalent activation energies for both probe wavelengths (within ±2 kJ/mol, the approximate accuracy limit). The **VWWV** variant reveals the fastest kinetics of all studied peptides and the same two-state-like behavior as the tyrosine variants. The conformational dynamics of the **WVVW** variant (Figure 5C) is different and resembles more that of **WWWW**, for which the strand and disorder relaxation times cannot be differentiated within the data accuracy at temperatures above ∼40 °C, making their high temperature behaviors two-state-like. By contrast, below 40 °C there is a clear differentiation in strand and disorder kinetics for **WWWW**, which is also obvious in the Arrhenius plot (Supporting Information) and reveals the existence of folding intermediates. Likewise, the relaxation times of **WVVW** also become differentiated but at a lower temperature (below ∼20 °C) than for **WWWW** (Figure 5C). The much lower E_a determined for **WVVW** (12.8 kJ/mol) as compared to **WWWW** (27.8 kJ/mol) (Table 3) is probably less reliable due to the reduced number of measurable data points for the Arrhenius fit.

Mechanistic Model. This variation in β-strand kinetics between **WWWW**, **YWWY**, and **VWWV** suggests that the stabilization provided by aromatic (Trp−Trp or Tyr−Trp) versus purely hydrophobic (Val−Val) interactions result in different mechanisms of unfolding due to the relative strengths

dx.doi.org/10.1021/jp506658x | J. Phys. Chem. B 2014, 118, 14234−14242

of their cross-strand contacts. In this section, we compare potential mechanisms for **WWWW** with its variants.

The **WWWW** peptide unfolding has an intermediate where the four Trps retain cross-strand interaction at higher temperatures and thus stabilize substantial structure and local H-bonds in the center of the hairpin, while the ends and the turn become more disordered, losing their cross-strand H-bonds. This more structured **WWWW** intermediate favors a multistate unfolding process (as shown by the red and blue lines in Figure 5 plots). The next step in **WWWW** unfolding is presumably to form a second intermediate with just one pair of Trps interacting, resulting in substantial fraying of the strand. The Trps by the turn may lose their interaction first, but our data suggest the Trp interaction on the strand termini are more likely to be lost.

For **YWWY**, there is a weaker edge-to-face aromatic interaction with only Tyr close to the termini than with **W**, as in **WWWW**. At a temperature sufficient to break the stronger Trp−Trp interaction, the weaker Tyr−Tyr one may already be broken or be too weak to hold the hairpin together. In this case, the Trp−Trp interaction would aid the Tyr−Tyr one in stabilizing the cross-strand H-bonds and β-structure, but when the Trp−Trp is lost, the whole hairpin would open. In this case, only a minimal population of any intermediate, presumably one with residual Trp−Trp contact, would occur. This could result in a process that experimentally appears, with IR monitoring of the strand conformation, to be two-state, the strand and disorder kinetics having the same thermal behavior (Figure 5A).

On the other hand, for **VWWV,** with Val close to the termini and lacking the stronger aromatic interaction, maintaining the strand conformation depends on the cross-strand H-bonds and the relatively weak van der Waals attraction of Val residues. The turn is stabilized by the remaining two cross-strand Trp residues, but the termini lack added aromatic stabilization, so that at low temperatures the hairpin is folded but at higher temperatures the strand termini fray to a larger extent. This can lead to formation of a substantially populated ensemble of intermediate states that are more like the unfolded state with few H-bonds but with some aspect of the turn remaining. Consequently, for **VWWV**, the weaker aliphatic interaction, only hydrophobic with no aromatic contribution, results in a less stable structure, with more fraying and faster kinetics (Figure 5B).

By contrast, for the varients with Trp at the terminal positions, a different mechanism dominates. The **WYYW** variant behaves very much like the **YWWY** one with similar rates and an apparent two-state behavior, to our level of sensitivity. In these cases, overcoming the Trp−Trp interaction, which is more stable than Tyr−Tyr, leads to simultaneous break down of the H-bonded interstrand interaction, which is not sufficient to stabilize the hairpin at higher temperatures. The result is apparent two-state behavior.

For **WVVW**, rates similar to those of **WYYW** are observed at high temperatures but the kinetics diverge at lower temperatures in contrast to **WYYW**, with the loss of sheet faster than gain of disorder (Figure 5C). This suggests that the Trp−Trp interaction stabilizes the termini while the strand structure is partially lost, unwinding from the turn in this case, as temperature is increased, resulting in a different mechanistic path than postulated above.

Most kinetics studied for the hairpin variants are faster than for the parent **WWWW** but counterintuitively have higher activation energies (Table 3). These differences are small, but the trends are consistent and outside the error limits. Using transition state theory, the free energy of activation $\Delta G^{\#}$ can be divided into an entropic and an enthalpic part:

$$k(T) = k_o \exp(-\Delta G^{\#}/RT) = k_o \exp(\Delta S^{\#}/R) \exp(-\Delta H^{\#}/RT) \quad (1)$$

In this model, E_a is included in the enthalpy of activation, $\Delta H^{\#} = E_a - RT$, which when increased reduces the rate constant, k. The pre-exponential factor, in turn depends on $\Delta S^{\#}$, the entropy of activation. Thus, given their higher E_a values, which should reduce the rates, the apparent rate enhancement for the mutants must be due to the entropic contribution, particularly for the rate-determining steps. The mutation of a cross-strand Trp pair makes the hairpin structure more flexible and increases the conformational space of the transition states. The dependence on $\Delta S^{\#}$ implies that the transition state must be at least partially unfolded, which would suggest that the weaker (non-Trp−Trp) cross-strand interaction is lost in the transition state or intermediate with the larger activation energy (rate-determining step in the process). Thermodynamic analysis of equilibrium FTIR data showed that some of the tyrosine and valine mutants have higher and some have lower ΔS values compared to Trpzip2. If we assume the final states are fully disordered, this would imply the initial states differ in order. However, our NMR structures do not support this, making these ΔS values difficult to rationalize and suggesting that the final states are not equivalently disordered.[12,13] The pattern indicates the faster rate of sheet loss for **VWWV** with the Val substitution depends on its having a transition state that is substantially disordered (i.e., closer to the final unfolded state). This would fit the increased fraying expected for the **VWWV** structure. However, in this case, the E_a values are less reliable because only low temperature kinetic data could be determined.

All the Tyr mutants have E_a greater than for **WWWW** and also have predominantly faster rates, which are additionally very similar for the loss of sheet and gain of disorder. Thus, the **WWWW** transition state must be more ordered than for the Tyr mutant ones, yet the Tyr mutants must have similar $\Delta S^{\#}$ changes in their transition states, even though the site of substitution changes among them. If formation of the **WWWW** intermediate with both Trp−Trp cross-strand interactions intact is rate determining for the parent Trpzip2, then $\Delta S^{\#}$ for that step might be significantly lower than for the transitions with either the Val or Tyr mutants we have studied. This difference could explain the relative variation in their T-jump relaxation rates. Such a mechanistic picture suggests the aromatic−aromatic interactions are similar in quality following a Tyr−Trp substitution but are overall weaker with Tyr, consequently destabilizing more fully folded transition states and favoring more disorder in the transition state. Unfolding would require more energy to break up more H-bonds and the hydrophobic interactions, but this could still result in faster kinetics due to the gain in entropy.

Impact on Folding Mechanism. In an attempt to illustrate the overall impact of the various mutations and their relative energetics on the folding mechanism, we have postulated a simplified reaction coordinate diagram isolating these qualitative aspects of that part of the potential surface important for the unfolding process (Figure 6). In **WWWW** (blue curve), the folded state first loses sheet cross-strand H-

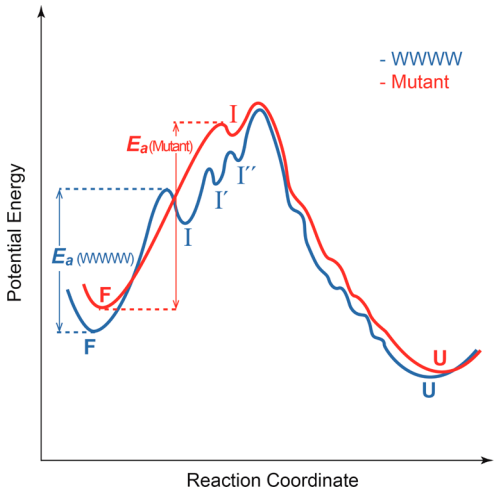

Figure 6. Proposed change in the qualitative folding energy landscape when hydrophobic interactions are modified (not to scale). The blue curve indicates the lower E_a and more organized transition state for the rate-determining step in the **WWWW** unfolding, whereas the red trace is a possible alteration when two Trps are substituted with Tyr resulting in a higher E_a but a more disorganized transition state.

bond structure on the termini and near the ends, creating an intermediate form. Once formed, the system can then unfold in a second or, more likely, in multiple steps through other intermediates having single pairs of Trp−Trp contacts and fewer cross-strand H-bonds to eventually form an unfolded state. The rate-determining step is that to the first intermediate and has a reduced E_a because the hydrophobic contacts and central H-bonds from the folded form remain in the transition state, indicating little loss of energetic components.

The mutated forms do not show this intermediate, because the single Trp−Trp coupling is insufficient to stabilize a structure with strands maintaining these central cross-strand H-bonds. Due to the less consistency in the Val kinetics, we address the Tyr variant here. This can be most consistently seen for the **YWWY** case. Here the structure most likely unzips from the termini, leaving an intermediate with just a residual Trp−Trp contact close to the turn. This results in a higher energy transition state but one which is much less structured. This transition would lead to an intermediate or directly to an unfolded product possibly sampling various significantly unfolded states on a downhill route to the final state (red curve). Thus, the activation energy is larger for these mutants than for **WWWW** because most stabilizing interactions need to be broken, and the process seemingly would appear to be two-state to the observer.

CONCLUSION

Our kinetic study demonstrates the enormous potential of hydrophobic residues in modifying folding pathways. Measurements with mutant variants of the Trpzip2 β-hairpin peptide indicate that the hydrophobic residues can indirectly modulate the enthalpic and entropic contributions to the rate and thus result in major variations of the folding mechanism. Substitutions of tryptophans with either tyrosines or valines revealed that the potential surface depends critically on the residue−residue interaction, as we have probed by site-specific conformational dynamics. Although this 12-amino acid peptide is small in comparison to proteins, it can be regarded as a well-defined folding unit that might occur within a protein. Even if the modification of the potential surface is small, changing the barriers only slightly can have a large effect and could critically influence if the sequence would fold into the biologically active structure or to a misfolded and dysfunctional one.

ASSOCIATED CONTENT

Supporting Information

Figures of transient relaxation kinetics at several temperatures for the five mutants of Trpzip2, tables of the resulting relaxation times, the Arrhenius plot for Trpzip2C (WWWW), and the fit function for T_m determination are provided in a Supporting Information file. This material is available free of charge via the Internet at http://pubs.acs.org.

AUTHOR INFORMATION

Corresponding Authors

*E-mail: Karin.Hauser@uni-konstanz.de.
*E-mail: tak@uic.edu.

Notes

The authors declare no competing financial interest.

ACKNOWLEDGMENTS

We gratefully acknowledge financial support by the Deutsche Forschungsgemeinschaft (SFB 969 to K.H.) and by the Alexander von Humboldt Foundation (Humboldt Research Award to T.A.K.) and National Science Foundation (CHE07-18543 to T.A.K.).

REFERENCES

(1) Cochran, A. G.; Skelton, N. J.; Starovasnik, M. A. Tryptophan Zippers: Stable, Monomeric β-Hairpins. *Proc. Natl. Acad. Sci. U.S.A.* **2001**, *98*, 5578−5583; *Correction: Proc. Natl. Acad. Sci. U.S.A.* **2002**, *5599*, 9081−9082.

(2) Guvench, O.; Brooks, C. L. Tryptophan Side Chain Electrostatic Interactions Determine Edge-to-Face Vs Parallel-Displaced Tryptophan Side Chain Geometries in the Designed Beta-Hairpin "Trpzip2". *J. Am. Chem. Soc.* **2005**, *127*, 4668−4674.

(3) Wu, L.; McElheny, D.; Setnicka, V.; Hilario, J.; Keiderling, T. A. Role of Different Beta-Turns in Beta-Hairpin Conformation and Stability Studied by Optical Spectroscopy. *Proteins: Struct., Funct., Bioinf.* **2012**, *80*, 44−60.

(4) Smith, A. W.; Chung, H. S.; Ganim, Z.; Tokmakoff, A. Residual Native Structure in a Thermally Denatured β-Hairpin. *J. Phys. Chem. B* **2005**, *109*, 17025−17027.

(5) Jones, K. C.; Peng, C. S.; Tokmakoff, A. Folding of a Heterogeneous Beta-Hairpin Peptide from Temperature-Jump 2D IR Spectroscopy. *Proc. Natl. Acad. Sci. U. S. A.* **2013**, *110*, 2828−2833.

(6) Yang, W. Y.; Gruebele, M. Detection-Dependent Kinetics as a Probe of Folding Landscape Microstructure. *J. Am. Chem. Soc.* **2004**, *126*, 7758−7759.

(7) Yang, W. Y.; Pitera, J. W.; Swope, W. S.; Gruebele, M. Heterogenous Folding of the Trpzip Hairpin: Full Atom Simulation and Experiment. *J. Mol. Biol.* **2004**, *336*, 241−251.

(8) Snow, C. D.; Qiu, L.; Du, D.; Gai, F.; Hagen, S. J.; Pande, V. S. Trp Zipper Folding Kinetics by Molecular Dynamics and Temperature Jump Spectroscopy. *Proc. Natl. Acad. Sci. U.S.A.* **2004**, *101*, 4077−4082.

(9) Hauser, K.; Krejtschi, C.; Huang, R.; Wu, L.; Keiderling, T. A. Site-Specific Relaxation Kinetics of a Tryptophan Zipper Hairpin Peptide Using Temperature-Jump IR-Spectroscopy and Isotopic Labeling. *J. Am. Chem. Soc.* **2008**, *130*, 2984−2992.

(10) Hauser, K.; Ridderbusch, O.; Roy, A.; Hellerbach, A.; Huang, R.; Keiderling, T. A. Comparison of Isotopic Substitution Methods for Equilibrium and T-Jump Infrared Studies of β-Hairpin Peptide Conformation. *J. Phys. Chem. B* **2010**, *114*, 11628−11637.

(11) Davis, C. M.; Dyer, R. B. Dynamics of an Ultrafast Folding Subdomain in the Context of a Larger Protein Fold. *J. Am. Chem. Soc.* **2013**, *135*, 19260−19267.
(12) Wu, L.; McElheny, D.; Huang, R.; Keiderling, T. A. Role of Tryptophan−Tryptophan Interactions in Trpzip Beta-Hairpin Formation, Structure, and Stability. *Biochemistry* **2009**, *48*, 10362−10371.
(13) Wu, L.; McElheny, D.; Takekiyo, T.; Keiderling, T. A. Geometry and Efficacy of Cross-Strand Trp/Trp, Trp/Tyr, and Tyr/Tyr Aromatic Interaction in a β-Hairpin Peptide. *Biochemistry* **2010**, *49*, 4705−4715.
(14) Takekiyo, T.; Wu, L.; Yoshimura, Y.; Shimizu, A.; Keiderling, T. A. Relationship between Hydrophobic Interactions and Secondary Structure Stability for Trpzip Beta-Hairpin Peptides. *Biochemistry* **2009**, *48*, 1543−1552.
(15) Roy, A.; Bour, P.; Keiderling, T. A. TD-DFT Modeling of the Circular Dichroism for a Tryptophan Zipper Peptide with Coupled Aromatic Residues. *Chirality* **2009**, *21*, E163−E171.
(16) Du, D.; Tucker, M. J.; Gai, F. Understanding the Mechanism of β-Hairpin Folding Via ϕ-Value Analysis. *Biochemistry* **2006**, *45*, 2668−2678.
(17) Huang, R.; Wu, L.; McElheny, D.; Bour, P.; Roy, A.; Keiderling, T. A. Cross-Strand Coupling and Site-Specific Unfolding Thermodynamics of a Trpzip β-Hairpin Peptide Using 13C Isotopic Labeling and IR Spectroscopy. *J. Phys. Chem. B* **2009**, *113*, 5661−5674.
(18) Wray, W. O.; Aida, T.; Dyer, R. B. Photoacoustic Cavitation and Heat Transfer Effects in the Laser-Induced Temperature Jump in Water. *Appl. Phys. B: Laser Opt.* **2002**, *74*, 57−66.
(19) Rose, G. D.; Wolfenden, R. Hydrogen-Bonding, Hydrophobicity, Packing, and Protein-Folding. *Annu. Rev. Bioph. Biom.* **1993**, *22*, 381−415.